J Paleolimnol (2012) 48:9–26
DOI 10.1007/s10933-012-9607-4

ORIGINAL PAPER

A multi-proxy record of the Last Glacial Maximum and last 14,500 years of paleoenvironmental change at Lone Spruce Pond, southwestern Alaska

Darrell S. Kaufman · Yarrow Axford · R. Scott Anderson · Scott F. Lamoureux · Daniel E. Schindler · Ian R. Walker · Al Werner

Received: 8 September 2011 / Accepted: 17 March 2012 / Published online: 13 May 2012

Abstract Sediment cores from Lone Spruce Pond (60.007°N, 159.143°W), southwestern Alaska, record paleoenvironmental changes during the global Last Glacial Maximum (LGM), and during the last 14,500 calendar years BP (14.5 cal ka). We analyzed the abundance of organic matter, biogenic silica, carbon, and nitrogen, and the isotope ratios of C and N, magnetic susceptibility, and grain-size distribution of bulk sediment, abundance of alder shrub (*Alnus*) pollen, and midge (Chironomidae and Chaoboridae) assemblages in a 4.7-m-long sediment sequence from the depocenter at 22 m water depth. The basal unit contains macrofossils dating to 25–21 cal ka (the global LGM), and is interpreted as glacial-lacustrine sediment. The open water requires that the outlet of the Ahklun Mountain ice cap had retreated to within 6 km of the range crest. In addition to cladocerans and diatoms, the glacial-lacustrine mud contains chironomids consistent with deep, oligotrophic conditions; several taxa associated with relatively warm conditions are present, suggestive of relative warmth during the global LGM. The glacial-lacustrine unit is separated from the overlying non-glacial lake sediment by a possible disconformity, which might record a readvance of glacier ice. Non-glacial sediment began accumulating around 14.5 cal ka, with high flux of mineral matter and fluctuating physical and biological properties through the global deglacial period, including a reversal in biogenic-silica (BSi) content during the Younger Dryas (YD). During the global deglacial interval, the $\delta^{13}C$ values of lake sediment were higher relative to other periods, consistent with low C:N ratios (8), and suggesting a dominant atmospheric CO_2 source of C for phytoplankton. Concentrations of

This is one of 18 papers published in a special issue edited by Darrell Kaufman, and dedicated to reconstructing Holocene climate and environmental change from Arctic lake sediments.

D. S. Kaufman (✉) · R. S. Anderson
School of Earth Sciences and Environmental Sustainability, Northern Arizona University, Flagstaff, AZ 86011, USA
e-mail: darrell.kaufman@nau.edu

Y. Axford
Department of Earth and Planetary Sciences, Northwestern University, Evanston, IL 60208, USA

S. F. Lamoureux
Department of Geography, Queen's University, Kingston, ON K7L 3N6, Canada

D. E. Schindler
School of Aquatic and Fishery Sciences, University of Washington, Seattle, WA 98195, USA

I. R. Walker
Department of Biology, University of British Columbia Okanagan, Kelowna, BC V1V 1V7, Canada

A. Werner
Department of Geology and Geography, Mount Holyoke College, South Hadley, MA 01075, USA

aquatic faunal remains (chironomids and Cladocera) were low throughout the deglacial interval, diversity was low and warm-indicator taxa were absent. Higher production and air temperatures are inferred following the YD, when bulk organic-matter (OM) content (LOI 550 °C) increased substantially and permanently, from 10 to 30 %, a trend paralleled by an increase in C and N abundance, an increase in C:N ratio (to about 12), and a decrease in $\delta^{13}C$ of sediment. Post-YD warming is marked by a rapid shift in the midge assemblage. Between 8.9 and 8.5 cal ka, *Alnus* pollen tripled (25–75 %), followed by the near-tripling of BSi (7–19 %) by 8.2 cal ka, and $\delta^{15}N$ began a steady rise, reflecting the buildup of N and an increase in denitrification in soils. Several chironomid taxa indicative of relatively warm conditions were present throughout the Holocene. Quantitative chironomid-based temperature inferences are complicated by the expansion of *Alnus* and resulting changes in lake nutrient status and production; these changes were associated with an abrupt increase in cladoceran abundance and persistent shift in the chironomid assemblage. During the last 2,000 years, chironomid-assemblage changes suggest cooler temperatures, and BSi and OM values were generally lower than their maximum Holocene values, with minima during the seventh and eighth centuries, and again during the eighteenth century.

Keywords Quaternary paleoenvironments · Lake Sediment · Alaska · Midges · Pollen · Biogenic silica · Magnetic susceptibility · Carbon and nitrogen isotopes

Introduction

We present a record of paleoenvironmental change inferred from lake sediment at Lone Spruce Pond, located in the northern Bristol Bay region of southwestern Alaska (Fig. 1). We describe multiple physical, biogeochemical, and biological properties of a 4.7-m-long sediment sequence that extends back to the global Last Glacial Maximum (LGM). The multiproxy approach provides new insights into the paleoenvironment of this region during the global LGM, and during key transitions of the late glacial and Holocene. The approach reveals differences in the timing of changes, and insights into the interaction between climate change, catchment vegetation cover and runoff responses, and lake ecosystem changes. This includes the interval of rapid and dramatic expansion of alder (*Alnus*) shrubs centered around 8.6 cal ka, which transformed the landscape and impacted the nutrient status of Lone Spruce Pond. Comparison of the sedimentary record from Lone Spruce Pond with those from other lakes that have recently been studied in the area reveals the complexity of climate change impacts on different watersheds and on varying time scales.

Study site

Lone Spruce Pond (informal name; 60.007°N, 159.143°W) is located in the northeastern Ahklun Mountains, southwest Alaska, about 100 km northwest of Dillingham (Fig. 1) at the upper elevation limit of *Picea* in the region. Lone Spruce Pond is 135 m asl and 16 m above adjacent Lake Chuaekuktuli, one of the large fjord-like lakes extending from the eastern foothills of the Ahklun Mountains (Fig. 1). The surface area of Lone Spruce Pond is 0.05 km^2, and its maximum depth is 22 m (Fig. 2). The adjacent terrain is densely vegetated by shrubs of *Alnus viridis,* with some *Betula* and *Salix*. The surrounding hillslopes rise steeply from the pond, with the 0.14 km^2 watershed extending only a short distance beyond the shore. The outlet stream cascades over falls, precluding anadromous fish migration from Lake Chuaekuktuli, about 100 m to the east. In July 2009, a beaver dam across the outflow raised water level in the pond by about 1.5 m. Directly south of Lone Spruce Pond is Shadow Bay, the proximal sub-basin of Lake Chauekuktuli. Shadow Bay is separated from the main lake by a narrow, dissected arcuate ridge marked by abundant surface boulders, which we interpret as a late-glacial end moraine.

During the last glacial period, an ice cap formed over the central Ahklun Mountains, and an outlet glacier extended 55 km downvalley from Lone Spruce Pond (Fig. 1; Kaufman et al. 2011a). Modern glaciers are restricted to the highest north-facing cirques along the range crest, including the high massif located 6 km west of Lone Spruce Pond.

The modern climate of the Ahklun Mountains is transitional between maritime and continental (NOAA 1980). Mean annual temperature is 1 °C, with monthly

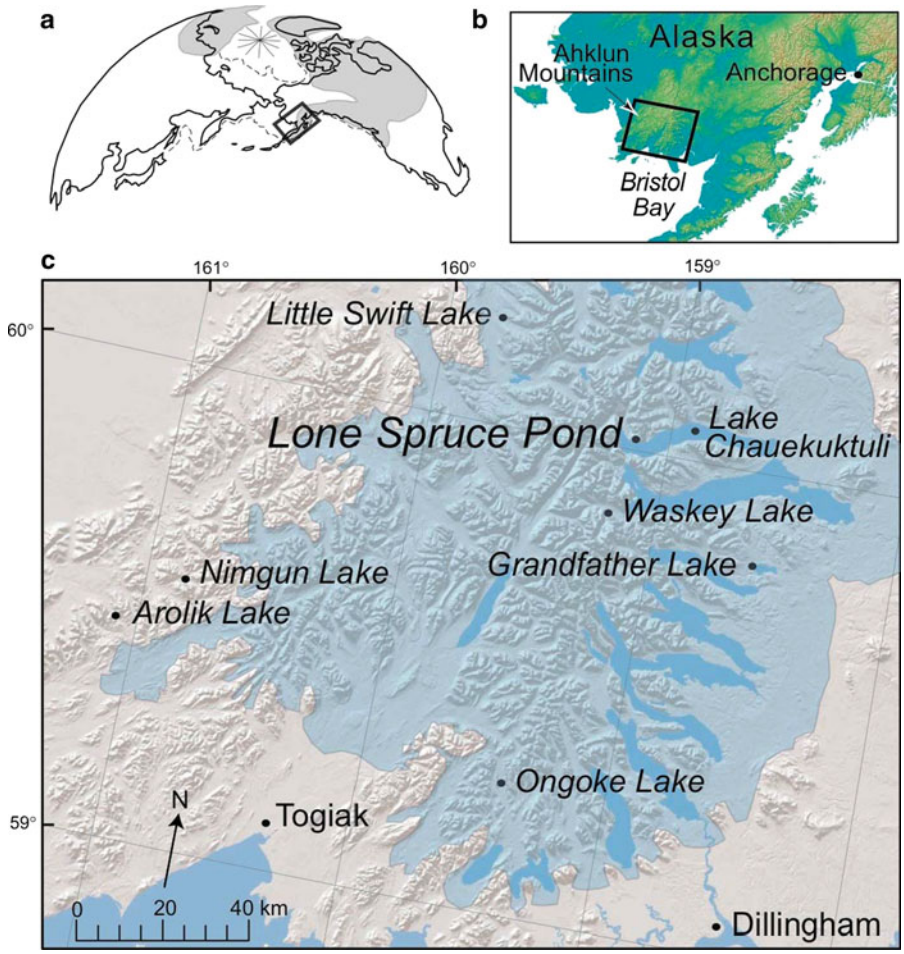

Fig. 1 Location of Lone Spruce Pond in context of **a** the Northern Hemisphere, showing the rough extent of ice sheets during the global Last Glacial Maximum (*gray area*) and the continental shelf break (*dashed line*); **b** southwest Alaska showing the Ahklun Mountains in the Bristol Bay region; and **c** the maximum extent of ice during the late Wisconsin (*light blue* area; from Kaufman et al. 2011a), and other previously studied lakes mentioned in the text. (Color figure online)

mean temperatures ranging from −9° (Jan) to 13 °C (Jul) (1971–2000; WRCC 2008) at Dillingham, located along the coast of northern Bristol Bay, 115 km southeast of Lone Spruce Pond. Precipitation peaks during late summer to early fall, with an average annual total of 650 mm. A meteorological station equipped with an Onset temperature/relative humidity sensor and rain gauge was deployed at Shadow Bay in August 2006 (data at http://jan.ucc.nau.edu/~dsk5/S_AK/). A comparison of mean daily air temperature (August 2006–2007) at Shadow Bay with temperature at Dillingham shows a strong correlation, suggesting that meteorological conditions at Shadow Bay are similar to the regional climatology (Kaufman et al. 2011b). Rainfall at Shadow Bay is less closely related to that at Dillingham, likely due to local factors typical of mountainous terrain.

Materials and methods

Water depths in Lone Spruce Pond were sounded using a drop line and interpolated using GIS software. The elevation of the pond above Lake Chuaekuktuli was measured repeatedly using an altimeter to determine their elevational difference. Sediment cores were taken from multiple sites in Lone Spruce Pond (Fig. 2). The longest continuous sediment sequence was recovered during April 2007 from site 3 (07-LSP-03) at a depth of 22 m. In July 2009, we reoccupied site 3 (to within several meters) to recover a surface core with a well-preserved sediment–water interface (09-LSP-4A). The cores were spliced using a 2-mm-thick, beige tephra bed present in both. The composite core is 4.7 m long and is referred to as LSP-3/4, the focus of this study. To ensure the water-rich core top

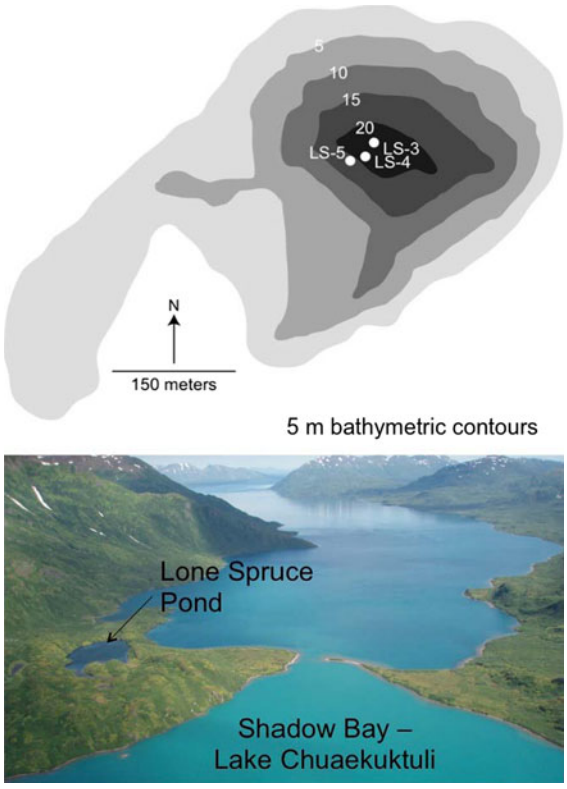

Fig. 2 **a** Bathymetric map of Lone Spruce Pond with core sites. **b** Aerial view of Lone Spruce Pond located 16 m above the level of Lake Chuaekuktuli. View is to the east, away from the mountain front. The spit separating Shadow Bay from the main body of Lake Chuaekuktuli is underlain by a bouldery ridge, which we interpret as a late-glacial moraine deposited sometime prior to 14.5 cal ka when non-glacial sediment began accumulating in Lone Spruce Pond

from the surface core would be preserved during travel, we split the core in the field, allowed the core face to dry slightly, and packaged each half with bundling film for shipment to the Sedimentary Records of Environmental Change Laboratory at Northern Arizona University (NAU), where they were stored at 4 °C.

In the lab, cores were described and magnetic susceptibility (MS) was measured along the core face at 0.5 cm intervals using a Bartington MS2 meter with a MS2-E surface-scanning sensor. Biogenic-silica (BSi) was extracted from 409 bulk sediment samples of which 32 were replicates using 10 % Na_2CO_3, and the concentration of SiO_2 was determined with a spectrophotometer following the procedure of Mortlock and Froelich (1989). Organic matter content (OM) was estimated for 230 samples by heating 0.1–1.4 g of dry sediment at 550 °C for 5 h. Grain size was measured on 205 samples using a Beckman Coulter LS200 particle size analyzer at the Environmental Variability and Extremes Laboratory at Queen's University. Each sample was pretreated with 35 % H_2O_2 and analyzed with sonication for 60 s three times and the third run was retained, unaveraged.

Total C and N concentration and isotope composition of 93 bulk-sediment samples was determined using an NC 2100 elemental analyzer (CE Instruments, Milan, Italy) connected to a Thermo-Finnigan Delta plus XL isotope ratio mass spectrometer (Thermo-Electron Corp., Bremen, Germany) at the Colorado Plateau Stable Isotope Laboratory, NAU. Prior to EA-IRMS analysis, non-acidified sediment samples were dried at 105 °C and homogenized by grinding with mortar and pestle. The $\delta^{13}C$ and $\delta^{15}N$ values were calculated using standard notations.

Pollen was analyzed from 118, 2-ml sediment samples, using a modified Fægri et al. (1989) procedure. Pollen grains were suspended in silicone oil and were identified under 400× magnification using the modern reference collection at the Laboratory of Paleoecology, NAU, and published sources. For this study, we focus on the relative abundance of alder (*Alnus*) pollen only. The growth of *Alnus* thickets across the local landscape was associated with the most prominent environmental change of the Holocene. The entire pollen record and the interpretation of the vegetation history at Lone Spruce Pond will be presented in a subsequent publication.

Midge remains (chironomid head capsules and *Chaoborus* mandibles) were processed following standard protocols (Walker 2001), sieved on a 100 μm sieve, and identified with reference primarily to Brooks et al. (2007) and Barley et al. (2006) (for Chironomidae), and Uutala (1990) (for Chaoboridae). Assemblage data are reported here for 29 samples that contained between 34 and 127 whole identifiable chironomid head capsules each; all but five of those samples contained at least 40 whole identifiable chironomid head capsules. Two additional samples from the basal 20 cm of the core yielded no chironomid or *Chaoborus* remains, and eight additional samples from elsewhere in the core yielded fewer than 20 head capsules; for these samples with count sums less than 20, only overall head capsule concentration (not assemblage composition) is reported here. To provide an additional downcore indicator of aquatic

conditions, the abundance of cladoceran remains in each sample was characterized qualitatively (as absent, low, moderate, or high).

Chironomid counting procedures and taxonomy were harmonized with the midge training set of Barley et al. (2006), which was developed based upon data from 145 lakes in northwestern North America including Alaska. Chironomid-inferred July air temperatures were modeled using three different regression methods for comparison: a two-component weighted averaging partial least squares (WA-PLS) model, a simple weighted averaging (WA) model without tolerance downweighting, and WA with tolerance downweighting. All three models used the same training set sites and square-root transformed chironomid species data. Both WA models employed inverse deshrinking. All models were run using the computer program C2 v 1.6.6 (Juggins 2003) and cross-validated by bootstrapping. Model statistics and site details are provided by Barley et al. (2006). Fossil taxa from Lone Spruce Pond are well represented in the modern calibration data, with only one minor taxon not represented in the training set (*Demicryptochironomus*, present in two downcore samples at <1 % abundance). To assess the appropriateness of training set sites as analogs for downcore samples, squared-chord distances (SCDs) were calculated between untransformed chironomid species data in each fossil sample and its nearest analog in the training set, using the modern analog technique (MAT). To objectively pinpoint major shifts in chironomid assemblages, assemblage zones were defined using stratigraphically constrained incremental sum of squares cluster analysis, employing the CONISS program packaged with TILIA v1.7.16, using Euclidean distance as a dissimilarity coefficient, and based upon chironomid (not Chaoboridae) taxa with maximum abundances >2 %.

The age model for the composite core (LSP-3/4) was constrained by 21 AMS ^{14}C ages on plant macrofossils, by a profile of the short-lived Pu isotopes through the near-surface sediment, and by tephrochronology, as described by Kaufman et al. (2012). Tephra layers are considered "instantaneous" deposits and the corresponding depths were removed from the core stratigraphy and the resulting age model. The age model was constructed by fitting the age-depth data with a smoothed spline using the *clam* code (Blaauw 2010). The routine uses IntCal09 (Reimer et al. 2004) to calibrate the ^{14}C ages to calendar years. All ages in the text are reported as calendar years prior to 1950 AD (cal BP or cal ka).

Results[1]

Sediment core geochronology

The age model for LSP-3/4 (Fig. 3), and the ^{14}C ages that were used to constrain it (Table 1), were published recently (Kaufman et al. 2012), and are summarized here. Three ^{14}C ages were analyzed from unit 1 (see below for unit descriptions). The two ages on vegetation macrofossils taken from 2 cm below the top of the unit, both within 1 cm of each other and sampled on two occasions are 25.4 and 21.3 cal ka. The age on bulk sediment (the only non-macrofossil analysis) from 20 cm below the other pair is 24.4 cal ka. We interpret these ages as finite. They indicate that glacial-lacustrine mud was accumulating in Lone Spruce Pond between around 21 and 25 cal ka. We cannot rule out the possibility that the dated macrofossils (and carbon-based substances that comprised the bulk-sediment age) were reworked from an older deposit into younger glacial-lacustrine sediment. Nonetheless, the macrofossils clearly date a time of non-glacial conditions in the catchment.

Two ^{14}C ages of 12.6 and 12.2 cal ka (stratigraphically reversed) were analyzed from unit 2 (Table 1). The samples were separated by 4 cm and were prepared and analyzed on two occasions. A second pair of samples from the base of unit 1, about 20 cm higher in the core, returned ^{14}C ages of 13.4 and 13.0 cal ka (also stratigraphically reversed). Similarly, the samples were separated by 4 cm and were analyzed on two occasions. The highly reproducible results indicate the integrity of the ^{14}C ages. Rather than inferring that the younger material was somehow injected into older sediment, we favor the more likely explanation that older material that overlies the younger ages includes older carbon. We therefore reject the older pair of ages. This interpretation is supported by the correlation of the 1-cm-thick tephra at 386 cm depth (2 cm below the younger pair of ages)

[1] All of the data from Lone Spruce Pond presented in this study are available on-line through the World Data Center for Paleoclimatology (http://www.ncdc.noaa.gov/paleo/pubs/jopl2012arctic/jopl2012arctic.html).

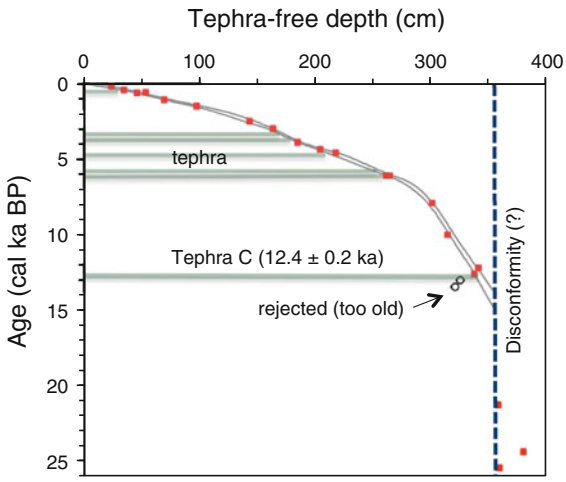

Fig. 3 Age-depth model for core LSP-3/4 from Lone Spruce Pond. The chronology is constrained by 22 AMS ^{14}C ages and is corroborated by the regional tephrochronology (Kaufman et al. 2012). Grey lines are 95 % confidence intervals as output by age-depth modeling routine, *clam* (Blaauw 2010). Data are listed in Table 1

with "Tephra C", which is dated at 12.5 cal ka at Arolik Lake (Kaufman et al. 2003), and which is geochemically and morphologically similar (Kaufman et al. 2012).

In addition to the two rejected ages, 15 samples ranging from 10.0 to 0.2 cal ka (from 357 to 24 cm depth) were analyzed for ^{14}C from unit 3. These ages were combined with the two accepted ages from unit 2, and with the Pu-based age for the onset of nuclear weapons testing, to derive an age-depth model for the composite core (Fig. 4). The 'R' code, *clam* was used to fit all 18 ages using a smooth spline (level of smooth = 0.3 (default); number of iterations = 10,000; Blaauw 2010). The average uncertainty associated with this age model, as evaluated at 1 cm intervals between the surface and the lowest ^{14}C-dated level in unit 2, is ± 109 year (2σ). The model assigns an age of 3.4 ± 0.1 cal ka to the base of the thickest (18 cm), coarsest tephra, which is identified as erupted from Aniakchak volcano (Kaufman et al. 2012), and is within the range of ages previously assigned to the eruption (e.g. Béget et al. 1992). The age model shows a major inflection at around 8.0 cal ka. Sedimentation rates increase by a factor of four above this level (0.1 vs. 0.4 mm year^{-1}), not including the tephra beds. The flux of mineral matter also increases following the expansion of *Alnus* (see below).

The age-depth model was extrapolated to the base of unit 2, where it reaches 14.5 ± 0.6 cal ka. On this basis, and assuming that the dated material in unit 1 was not reworked, the sedimentary sequence includes a possible disconformity representing about 6,000 years, which is marked by an oxidized zone formed into the top of unit 1.

Sediment core stratigraphy

Core LSP-3/4 contains eight visually obvious tephra beds, all with high MS values (Fig. 4). The tephra beds range in thickness from 0.2 to 18.0 cm and are beige or gray, with grain sizes ranging from fine ash to fine sand. The major-element geochemistry of glass from the tephra beds ranges from basaltic andesite to rhyolite (Kaufman et al. 2012). In addition to tephra beds, core LSP-3/4 comprises three lithologic units (Figs. 4, 5):

Unit 1 extends from the base of the core (477 cm) to 399 cm (~25–22 cal ka). It is gray, clay-rich mud, bedded in places, with abundant angular pebbles (<0.5 cm diameter). The upper surface of unit 1 is marked by an oxidized zone. MS values are generally high and variable (averaging 34 ± 17 SI). Clay content is high (44 ± 9 %), as is bulk density (1.0 ± 0.2 g cm^{-3}). Organic-matter and biogenic silica contents are low (OM = 5 ± 2 %; BSi = 2 ± 1 %), both with increasing-upward trends. We interpret this unit as glacial-lacustrine mud. The oxidized zone with pebbles might mark an unconformity.

Unit 2 extends from 399 to 371 cm (14.6–11.1 cal ka) and is composed of sandy mud. MS values are generally high and variable (42 ± 16 SI, excluding the 4-cm-thick zone of tephra-bearing sediment with MS values >100 SI). Mineral and organic constituents are also more variable than in units 1 or 3. Clay content is relatively low (18 ± 5 %), and sand content is relatively high (17 ± 12 %). OM and BSi contents are intermediate compared with units 1 and 3 (OM = 10 ± 4 %; BSi = 12 ± 4 %). We interpret this unit as lacustrine sediment with a significant proportion of hillslope-derived sediment.

Unit 3 extends from 371 cm to the surface (11.1 to 0 cal ka), comprising most (78 %) of the core. It is made of dark-brown, silt- and organic-rich mud (gyttja). Background MS values are consistently low (2 ± 3 SI, excluding the tephra beds). Silt dominates the grain-size distribution (77 ± 4 %). OM and BSi together make up over half of the mass of the

Table 1 Radiocarbon (^{14}C) ages, Lone Spruce Pond

Core	Midpoint depth (cm)										
	Tube	Below lake floor	Tephra-free	Sample thickness (cm)	AMS Lab ID	Lab #	^{14}C age (BP)	±	Calibrated age (BP)	±	Material
09-LSP-4A	0.8	0.8	0.8	0.5	–	–	–	–	−3	10	Pu onset
07-LSP-3	0.8	23.8	23.8	0.5	UCIAMS	37816	200	15	168	144	Leaf fragments
09-LSP-4A	35.1	35.1	34.9	0.2	UCIAMS	72311	360	60	406	86	Terrestrial leaf fragments; moss stems and leaves
07-LSP-3	23.3	46.3	46.1	0.5	UCIAMS	37817	595	15	607	41	Leaf fragments
09-LSP-4A	53.5	53.5	53.3	1.0	CAMS	144702	570	170	566	180	Unidentified
07-LSP-3	46.8	69.8	69.6	0.5	UCIAMS	37818	1150	15	1052	36	Leaf fragments
07-LSP-3	74.8	97.8	97.6	0.5	UCIAMS	37819	1600	25	1471	57	Leaf fragments
07-LSP-3	120.3	143.3	143.1	0.5	UCIAMS	37820	2435	35	2477	158	Leaf fragments
07-LSP-3	140.5	163.5	163.3	1.0	UCIAMS	37821	2875	15	2995	51	Leaf fragments
07-LSP-3	186.5	209.5	184.2	1.0	UCIAMS	37822	3575	20	3875	25	Leaf fragments
07-LSP-3	206.3	229.3	204.0	0.5	UCIAMS	37823	3905	15	4356	58	Leaf fragments
07-LSP-3	219.5	242.5	217.2	1.0	UCIAMS	37824	4090	15	4575	126	Leaf fragments
07-LSP-3	280.5	303.5	261.0	1.0	UCIAMS	72311	5320	15	6080	81	Woody fragments; moss stems and leaves
07-LSP-3	283.5	306.5	264.0	1.0	UCIAMS	37825	5330	15	6103	80	Leaf fragments
07-LSP-3	320.5	343.5	301.0	1.0	UCIAMS	37826	7075	15	7893	34	Unidentified
07-LSP-3	333.5	356.5	314.0	1.0	UCIAMS	83790	8910	120	9989	39	*Daphnia* egg case, *Juncus* seed, Bryophyte, Bryozoa
07-LSP-3	*340.0*	363.0	*320.5*	*2.0*	*UCIAMS*	*82294*	*11610*	*35*	*13440*	*71*	*Bryophyte, chitin, terrestrial leaf, woody fragments*
07-LSP-3	*344.5*	367.5	*325.0*	*1.0*	*UCIAMS*	*83791*	*11120*	*70*	*13002*	*98*	Daphnia, *Bryozoa*, Isoetes *spore, chitin*
07-LSP-3	356.5	379.5	337.0	1.0	UCIAMS	83792	10620	30	12584	29	Bryophyte stems, unidentified vegetation
07-LSP-3	360.0	383.0	340.5	2.0	UCIAMS	82295	10330	60	12176	167	Aquatic moss, chitin
07-LSP-3	379.0	402.0	358.5	2.0	CAMS	144698	17740	2680	21271	3224	Unidentified
07-LSP-3	379.5	402.5	359.0	1.0	UCIAMS	72309	21260	2100	25431	2522	Woody fragments; moss stems
07-LSP-3	400.0	423.0	380.1	2.0	CAMS	144828	20440	80	24385	141	Bulk sediment

Calibrated ages are the median of the probability density function (Telford et al. 2004); age uncertainty is one-half of the 1-sigma calibrated age range

Uppermost age is based on the onset of Pu deposition (see Kaufman et al. 2012)

Samples in italic were excluded from the age model for reasons discussed in the text

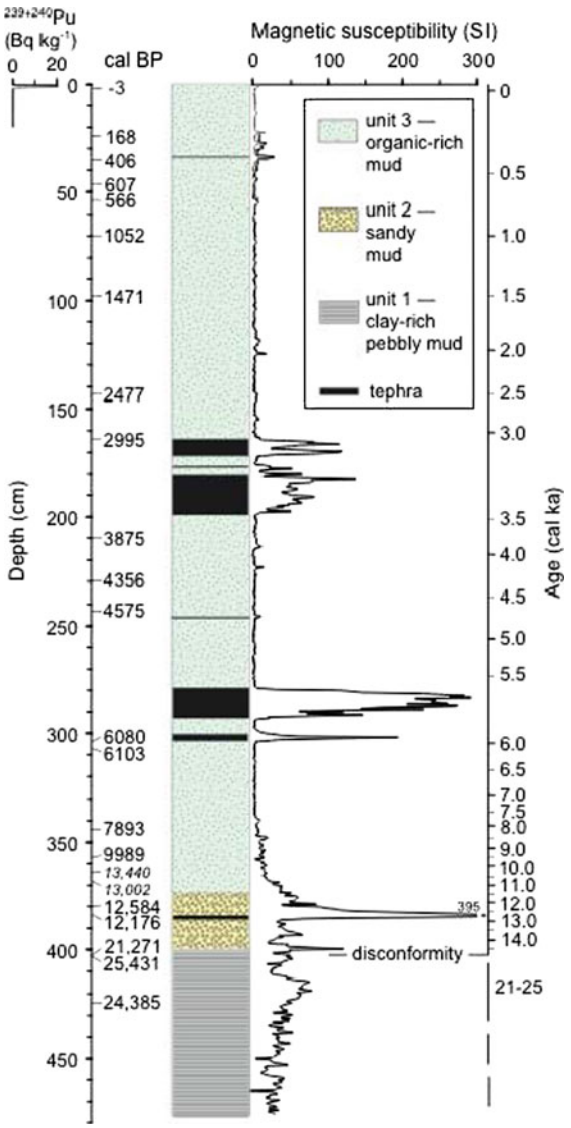

Fig. 4 Lone Spruce Pond stratigraphic sequence with $^{239+240}$Pu profile, ^{14}C ages (Table 1), and magnetic susceptibility (MS) profile (07-LS-3). Grey MS profile is from the surface core (09-LS-4A). The age-depth model (Fig. 3) was used for the right-hand scale

sediment (OM = 38 ± 4 %; BSi = 26 ± 5 %), but the two constituents show different trends over the lower quarter of the unit. OM increases from 10 to 30 % over the lower 5 cm of the unit, whereas BSi remains relatively low (around 10 %) over the lower 25 cm, then increases step-wise (by 15 %) at 344 cm (8.2 cal ka). We interpret this unit as lacustrine sediment of a lake similar to the present-day.

Midges

The two deepest samples analyzed from the Last Glacial Maximum (stratigraphic unit 1) yielded no midge or cladoceran remains, but samples from the upper half of unit 1 yielded concentrations exceeding those of the deglacial period (unit 2) and comparable to some samples from the Holocene (unit 3) (Fig. 6). Chironomid assemblages in this zone are dominated by *Heterotrissocladius* and Tanytarsini including *Micropsectra*. The unit contains taxa with a wide range of temperature optima as reported by Barley et al. (2006), including Chironomini (*Microtendipes, Polypedilum, Sergentia* and *Stictochironomus)* and Orthocladiinae (*Zalutschia, Psectrocladius (Psectrocladius), Parakiefferiella nigra* and *Mesocricotopus)*. Cluster analysis indicates that the chironomid assemblage in the uppermost LGM sample is more similar to deglacial assemblages than to the older LGM assemblages (i.e. CONISS groups both samples into chironomid zone B; Fig. 6). The uppermost LGM sample also differs from older samples in that it contains *Chaoborus* mandibles, which were not considered in the cluster analysis. Chironomid assemblages from unit 1 have good analogs within the training set, as defined by SCDs <0.33 (the 75 % confidence interval of closest-analog SCDs within the training set). Chironomid-based July summer air temperature reconstructions from unit 1 range widely between models, in terms of both absolute values and trends. Estimates range from ~9.5 °C for the WA model without tolerance downweighting to ~12.5 °C for the WA-PLS model.

Unit 2 is characterized by generally low concentrations of chironomids and Cladocera. Chironomid concentrations in the upper part of unit 2, which dates to the Younger Dryas, were too low to yield statistically significant numbers of head capsules, so only concentration (not assemblage) data are reported for this part of the record (Fig. 6). Assemblages within the lower portion of unit 2 are grouped together in the cluster analysis in zone B, along with the adjacent sample from unit 1. These assemblages are dominated by *Heterotrissocladius* and the Tanytarsini, with *Protanypus* and Orthocladiinae (including *Mesocricotopus, Corynoneura, Psectrocladius* and *Zalutschia*) also occurring. Chironomini are absent except for *Stictochironomus*. Chironomid assemblages from the

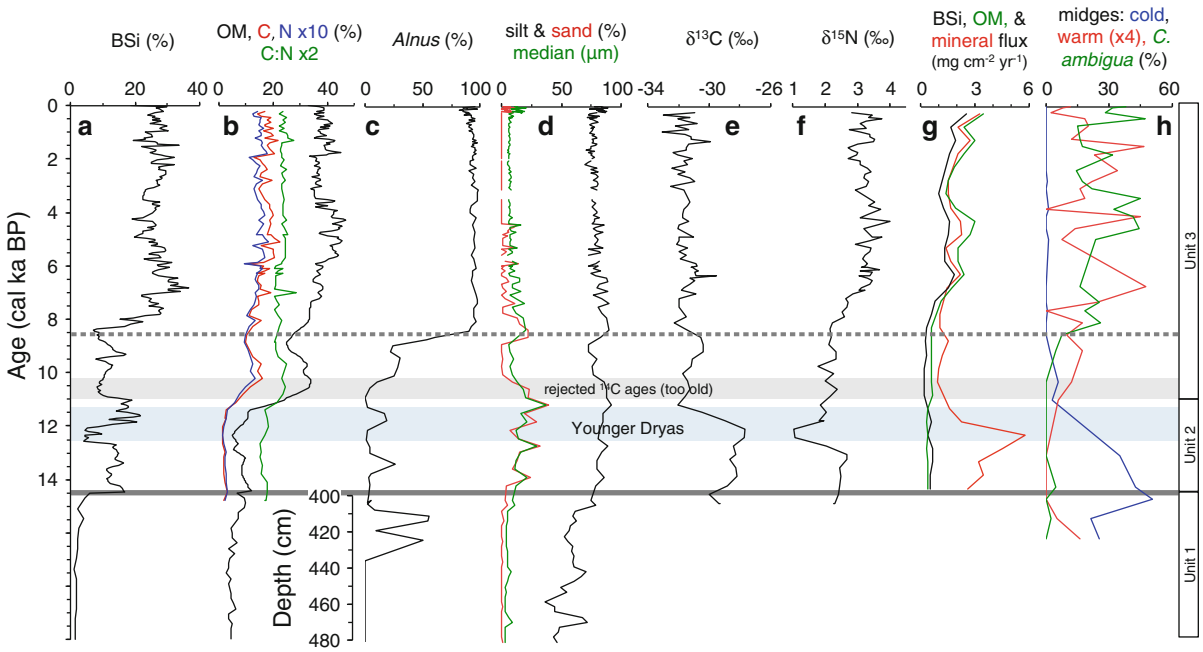

Fig. 5 Multiproxy records from Lone Spruce Pond core LSP-3/4. **a** Biogenic silica (BSi) content. **b** Organic matter (OM) content measured by loss on ignition, and C and N content determined by mass spectrometry. **c** *Alnus* pollen relative to total count. **d** Particle-size distribution, including the proportion of sand, silt, and median grain size. **e** C isotope value (standard notation). **f** N isotope value (standard notation). **g** Flux values for BSi, OM, and mineral matter. **h** Midge relative abundance including "cold indicator" species (*Heterotrissocladius*), "warm indicator Chironomini" (*Glyptotendipes, Polypedilum, Phaenopsectra flavipes, Cladopelma, Microtendipes, Dicrotendipes*), and *Corynocera ambigua.* Data plotted by depth (blf) below the possible disconformity (*gray line*); age-depth model from Fig. 3, excluding tephra beds. Major expansion of *Alnus* at 8.6 cal ka marked by dotted gray line

lower portion of unit 2 have good modern analogs as defined by SCDs. Temperature reconstructions from unit 2 vary by model as in unit 1. However, despite the relatively low abundance and diversity of Chironomini, assemblages from unit 2 overall suggest slightly warmer temperatures than in unit 1, with a minimum July air temperature estimate of 10.7 °C.

The chironomid assemblage changes markedly with the transition to unit 3 (and chironomid zone C): *Heterotrissocladius* is much less abundant and *Stictochironomus* is no longer present, along with an increase in the diversity of Chironomini and Orthocladiinae, and abundance of Chironomini including *Sergentia*. The bottom portion of unit 3 also contains very abundant *Chaoborus* remains, including *C. trivittatus* and *C. americanus* types. Chaoboridae disappear from the assemblage above 364 cm (10.4 cal ka). Cladocera are present throughout unit 3 and exceptionally abundant in the middle portion of the unit, beginning with the *Alnus* increase and subsequent BSi rise at 344 cm (8.2 cal ka). The chironomid assemblage undergoes a similarly pronounced change above the *Alnus* increase, with the transition to chironomid zone D, in which *Limnophyes, Corynoneura,* and *Corynocera ambigua* become more important, *Stempellinella/Zavrelia* and *Tanytarsus chinyensis* appear, and *Micropsectra* declines. The late Holocene chironomid zone E is characterized by the rise of *Sergentia*, continued abundance of *C. ambigua* and decline of *Micropsectra*, and later the return of *Stictochironomus*. Chironomid assemblages from the early Holocene chironomid zone C (below the rise of *Alnus* and BSi) have good to weak analogs within the training set. Temperature inferences for the early part of zone C are similar to those for the late glacial. All three models reconstruct a rise in temperature during the *Alnus* rise, followed by sustained temperatures between 11.0° and 12.5 °C throughout the remainder of the record. However, many assemblages from the middle and late Holocene (chironomid zones D and E, during and after

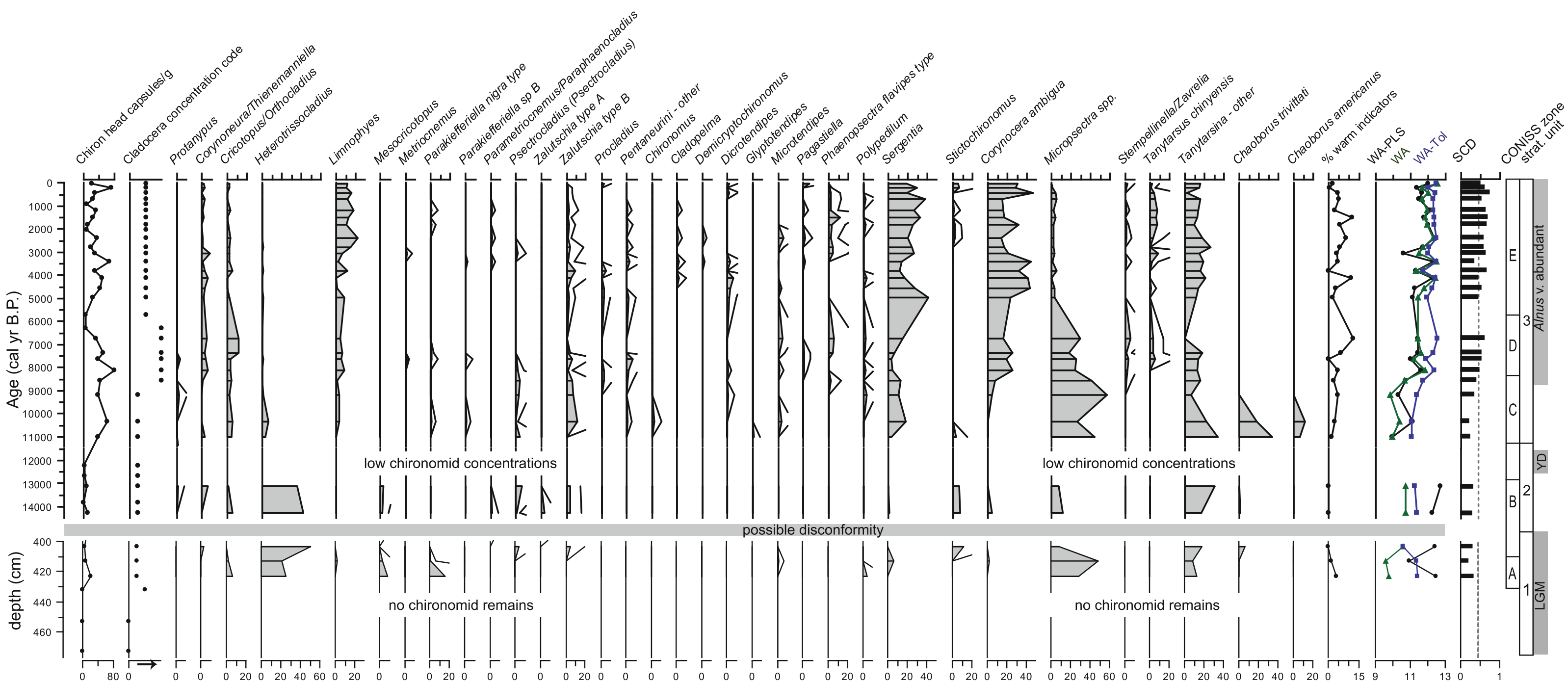

Fig. 6 Midge results plotted versus age for samples above the possible disconformity, and depth for Last Glacial Maximum samples. From *left* to *right*: chironomid head capsule concentrations, index of Cladocera concentrations (with abundance increasing to the *right*), and chironomid and *Chaoborus* taxa expressed as percentages of the sum of identifiable chironomids; percentage of the assemblage composed of relatively warm indicator taxa (*Polypedilum*, *Phaenopsectra flavipes, Glyptotendipes, Microtendipes, Cladopelma* and *Dicrotendipes*) as inferred from the training set (Barley et al. 2006); modeled July air temperatures from weighted averaging (WA, green triangles), weighted averaging with tolerance downweighting (WA-tol, *blue squares*) and 2-component weighted-averaging partial-least-squares (WA-PLS, *black circles*); and squared-chord distances (SCDs) to the nearest modern analog (*vertical dotted line* represents the analog cutoff, 95 % CI of minimum SCDs within the training set). Columns to *right* of diagram indicate chironomid assemblage zones (*letters A–E*), stratigraphic units defined by sediment characteristics (*numbers 1–3*), and significant events or time periods mentioned in the text (the Last Glacial Maximum (LGM), the Younger Dryas (YD), and the portion of the record for which *Alnus* makes up >50 % of the pollen assemblage). (Color figure online)

Alnus encroachment) have no modern analogs (defined as SCDs >0.44, the 95 % CI of dissimilarities within the training set).

Discussion

The global Last Glacial Maximum

The dominance of clay- and silt-sized sediment and presence of angular pebbles, which we interpret as ice-rafted, together with the presence (albeit relatively low concentrations) of aquatic chironomids, cladocerans, pollen, and diatoms, suggests that unit 1 was deposited in a glacial-lacustrine setting. Low BSi (<4 %) suggests that the water was turbid and cold, with a short ice-free season. Low OM (<6 %) probably indicates low production within and around Lone Spruce Pond. We suggest that the unit was deposited in a large proglacial lake, prior to the downcutting of the moraine that encloses the outlet of Lake Chauekuktuli, when the enlarged Pleistocene lake encompassed Lone Spruce Pond (now 16 m higher in lake-surface elevation).

Assuming that the dated materials are approximately the same age as the sediment that encloses them, then the age of deglaciation at Lone Spruce Pond was a few thousand years younger than the cessation of glacial meltwater input at Arolik Lake, located 125 km southwest of Lone Spruce Pond (Kaufman et al. 2003). The somewhat earlier retreat at Lone Spruce Pond could have been facilitated by the exceptionally low-gradient valley bottom and deep, water-filled trough over which the outlet glacier might have rapidly retreated along a calving front. The early retreat of the Ahklun Mountains ice cap is consistent with ages of local LGM moraines in the Brooks Range of northern Alaska, which were stabilized as early as about 27–25 cal ka (Briner and Kaufman 2008), indicating that mountain glaciers there retreated while global ice volume reached its maximum. Regardless of whether the dated macrofossils are reworked, they record an interval of ice-free conditions at Lone Spruce Pond around 25–21 cal ka, during which time the outlet of the Ahklun Mountain ice cap must have retreated from the core site, which is located at least 60 km from its late Wisconsin limit and 6 km of the range crest (Fig. 1). The extent to which this retreat might have been caused by a reduction in winter precipitation is unclear, although Alaska was certainly more arid during the LGM, as expected when the Bering–Chukchi platform became exposed by eustatic sea-level lowering.

Midge assemblages from unit 1 are consistent with the restricted extent of the Ahklun Mountain ice cap in suggesting relatively moderate climatic conditions during the global LGM. Aquatic invertebrates were rare or absent in the lower part of unit 1, but in the upper part, concentrations of chironomids generally exceed average concentrations of the late glacial; and in one LGM sample, concentrations exceed some Holocene values. Assemblages during this period were dominated by taxa (e.g. *Heterotrissocladius*, *Micropsectra, Parakiefferiella nigra, Mesocricotopus*) consistent with cool to cold summers and oligotrophic conditions. However, LGM assemblages also included taxa like *Microtendipes, Polypedilum*, and *Chaoborus,* which are most abundant or only present in lakes with July air temperatures >10 °C in eastern Beringia today (Barley et al. 2006). Notably, these assemblages did not include indicators of extreme cold such as *Pseudodiamesa* or *Oliveridia/Hydrobaenus*, common in the Canadian Arctic Islands today (Barley et al. 2006).

The presence of plant macrofossils and the high percentage (up to 55 %) of *Alnus* pollen (Fig. 5) in the upper part of unit 1 suggest a local presence of a shrubby flora, a conclusion bolstered by the occurrence of other shrubby taxa (*Betula*, *Salix*, *Artemisia*; Anderson et al. unpub.), although the concentration of all pollen types is low. If *Alnus* was present locally, it could have been favored by continual exposure of mineral soil by solifluction and other periglacial processes on nearby steep slopes (Wilson et al. 1985), or by gravelly deposits of braided streams (Viereck and Little, 2007) produced during glacial retreat.

The paleoenvironmental evidence from Lone Spruce Pond adds to similar evidence from elsewhere in Alaska and northwestern Canada indicating summer temperatures during the global LGM were not much colder than present. For example, pollen-based reconstructions indicate that July temperatures were on average only about 4 °C lower during the global LGM (Viau et al. 2008), and that mean annual temperatures were similar to or slightly warmer than today in Alaska (Bartlein et al. 2011). The pollen data agree with the two chironomid-based reconstructions in western Alaska (from Zagoskin and Burial lakes) that extend

through the global LGM, and that indicate summer temperatures were about 3.5 °C lower than modern (Kurek et al. 2009a).

The proxy evidence for relative warmth in Alaska agrees with the output of climate models, including NCAR's Community Climate System Model (CCSM3), which simulates summer temperatures that were higher than modern in Alaska during the global LGM (Otto-Bliesner et al. 2006). The amount of summer warming simulated by the model is controlled by the amount of southerly flow into Alaska, which is modulated by the prescribed elevation of the ice sheet over North America. A large ice sheet strengthens the Aleutian low and the associated surface winds, enhancing the advection of warmer air poleward into Alaska. As suggested by the model, we hypothesize that, as the Laurentide Ice Sheet thickened to its LGM height, summer temperature increased and mountain glaciers retreated in Alaska.

Possible disconformity (glacier readvance (?) 21 to 14.5 cal ka)

A possible erosional disconformity separates the lower glacial-lacustrine mud from the overlying sandy mud. Assuming that the dated material from unit 1 is not reworked, then the age difference between unit 1 and unit 2 indicates a gap of 6,000 years. Possibly, this interval includes a readvance of the outlet glacier from the Ahklun Mountain ice cap, during which Lone Spruce Pond was again ice covered. This is consistent with the evidence from elsewhere in the Ahklun Mountains for a readvance or standstill around 20 cal ka (Briner and Kaufman 2008). No till is present in the core, however, to mark a readvance over the site. Alternatively, the disconformity might record an interval of lowered lake level and possibly desiccation. If Lone Spruce Pond was dry, then the level of Lake Chuaekuktuli must also have been below present because the level of the possible disconformity in Lone Spruce Pond is below the lake level of Lake Chuaekuktuli. Moisture levels were generally lower in Alaska prior to about 15 cal ka. For example, Birch Lake in central Alaska was about 18 m lower than present prior to 15 cal ka (Abbott et al. 2000).

Alternatively, the contact that separates the glacial-lacustrine mud from the overlying organic-rich mud is conformable. For this alternative, the pronounced shift in sedimentology and sedimentation rate between units 1 and 2 could record the lowering of lake level to below the threshold that separates Lone Spruce Pond from Lake Chuaekuktuli. Once isolated from Lake Chuaekuktuli, the pond no longer received glacier meltwater. In addition, we cannot exclude the possibility that the dated material was reworked into the glacial-lacustrine subbasin now occupied by Lone Spruce Pond sometime after around 21 cal ka and prior to 14.5 cal ka (base of unit 2).

The last global deglaciation (14.5–11.5 cal ka)

Non-glacial sedimentation (unit 2) began at Lone Spruce Pond 14.5 ± 0.6 cal ka, coinciding with a period of major global warming (the Bølling warm period), which began around 14.7 cal ka as dated in Greenland ice (Rasmussen et al. 2006). The "deglacial age" at Lone Spruce Pond is coincident with the marked warming and freshening of surface waters in the northeastern Pacific (Davies et al. 2011), and it overlaps within age uncertainties with a 12 °C stepwise increase in July temperature inferred from chironomids from Hanging Lake, northern Yukon Territory (Kurek et al. 2009b).

The multi-proxy record from Lone Spruce Pond adds to the growing body of evidence of rapid climate and environmental changes in southwestern Alaska during the global deglacial period (e.g. Hu et al. 2003, 2006; Kaufman et al. 2010). Prior to the YD, the BSi content of sediment from Lone Spruce Pond remained relatively low (around 12 %) and $\delta^{13}C$ was high (around −28 ‰), as expected for a high proportion of C derived from phytoplankton fixation of atmospherically derived CO_2. These records are similar to those from nearby Grandfather Lake (Hu et al. 1995, 2001), but they lack the pronounced increase in BSi between 14.0 and 13.5 cal ka found in the sediments from Arolik and Ongoke lakes (Hu et al. 2006). The OM content of Lone Spruce Pond sediment remained low (around 9 %) prior to the YD, indicating low production within the lake and its catchment. This is consistent with chironomid-inferred temperatures from the pond, which indicate that summers prior to the YD were cooler than during the Holocene (Fig. 6), as suggested by the dominance of cold-dwelling taxa, low head capsule concentrations, and a lack of *Chaoborus* remains. And it agrees with isotopic and pollen data from Grandfather Lake (Hu and Shemesh 2003) that indicate cooler conditions prior to than after the YD.

The beginning of the YD at 12.8 cal ka is marked by a pronounced shift (from 12 to 5 %) in BSi content of sediment from Lone Spruce Pond, during which BSi reverted to values similar to those in the glacial-lacustrine mud. A similar shift in BSi content has also been reported from all other lake sedimentary records in the region that extend through the YD period, including Grandfather Lake (Hu et al. 1995, 2001), Arolik Lake (Hu et al. 2003; Kaufman et al. 2003), Ongoke Lake (Hu et al. 2006), and Nimgun Lake (Hu et al. 2002). The record from Lone Spruce Pond is consistent with other isotopic and paleoecological evidence for decreased temperature, moisture, and production across the region during the YD (summarized by Hu et al. 2006), and with the age of the moraine that encloses Waskey Lake (Briner et al. 2002).

Biogenic silica content of Lone Spruce Pond sediment increased abruptly around 12 cal ka, during the middle of the YD. The shift coincides with a sharp decrease (from −28 to −32 ‰) in $\delta^{13}C$, suggesting an increase in loading of terrestrially derived organic matter to the lake, which would have increased the pCO_2 of the water and supplied phytoplankton with more terrestrially-derived carbon. At the same time $\delta^{15}N$ increased as would be expected from accumulation and processing of N in watershed soils, with subsequent delivery to the lake. Evidence for increased temperature and production during the second half of the YD has been documented in other records from across southern Alaska (Kaufman et al. 2010), including nearby Grandfather Lake (Hu and Shemesh 2003).

The decrease in $\delta^{13}C$ along with the increase in $\delta^{15}N$ and BSi during the middle of the YD is consistent with the increase in the percentage of *Alnus* pollen (from background level to 18 %; Fig. 5). Anderson and Brubaker (1986) mapped the distribution of *Alnus* pollen percentages in lake surface sediments across northern Alaska, noting that *Alnus* shrubs were locally present where *Alnus* pollen was higher than 15–20 % of the local pollen sum. If similar for southwest Alaska, the pollen data suggest that shrubs were present near Lone Spruce Pond for several centuries during the second half of the YD. The percentage of *Alnus* pollen was reduced to background levels during the millennium both prior to and following this interval. This pattern is broadly similar to the fluctuations in BSi, indicating a link between diatom production and the presence of *Alnus*.

The flux of mineral matter, calculated as the mass percent other than OM and BSi, and scaled to density and sedimentation rate, is high over the lower part of unit 2, where bulk density is high and sedimentation rates are low (Fig. 5). On the basis of five-century averages, mineral matter flux reached its highest value (2.8 mg cm^{-2} $year^{-1}$) from 12.5 to 12.0 cal ka. The high sediment flux and coarse grain size indicate abundant input from the adjacent slopes, perhaps reflecting a decrease in terrestrial vegetation and an increase in periglacial slope activity during the YD. Vesicular–arbuscular fungi in this interval (RSA, unpublished) further indicate the exposure of soils and erosion into the lake. Changes in mineral flux can explain some of the percent-wise OM and BSi trends within the deglacial period.

Onset of the Holocene (11.5–9.0 cal ka)

The OM content of Lone Spruce Pond sediment increased rapidly, from 10 to 30 %, during the millennium following the YD (11.5–10.5 cal ka), paralleled by an increase in C and N abundance, and in the C:N ratio, and a decrease in $\delta^{13}C$, all signaling the input of organic C of terrestrial origin (Meyers and Lallier-Vergés 1999). Concentrations of chironomid remains, which were low during the YD interval, are ~10 times higher in the oldest Holocene sample. The pronounced increase in OM content following the YD is similar to that found in other lake sediments in the Ahklun Mountains, including Nimgun Lake (Hu et al. 2002), Arolik Lake (Kaufman et al. 2003), and Little Swift Lake (Axford and Kaufman 2004). Isotopic and paleoecological evidence indicate that the increase in OM content coincides with an increase in regional temperature and moisture (Hu et al. 2006). The shift to lower BSi content at 11 cal ka is unexpected, however, and we suspect that the record might be compromised by dissolution.

Two reproducible ^{14}C ages were returned on samples composed mainly of aquatic organisms from the interval between 11 and 10 cal ka. These older-than-expected ages might indicate a flush of old dissolved organic carbon to Lone Spruce Pond that led to a reservoir effect. We speculate that the old C had previously been sequestered in frozen soils, which thawed during this period of significant warming.

Midge assemblages also underwent a major shift at the YD-Holocene transition, including the decline of

Heterotrissocladius and disappearance of *Stictochironomus*, increase in relative abundance of Chironomini, increase in overall chironomid diversity, and the appearance and short-lived very high abundance of *Chaoborus*. Many of these changes seem suggestive of an abrupt warming, although the temperature models do not indicate major warming at this time, perhaps due to the concurrent rise of *Micropsectra* (which has a relatively cool-temperature optimum but has previously been noted to be somewhat problematic taxonomically, as the morphotype may include several species with different environmental preferences) and the fact that the models consider only chironomids and not *Chaoborus*, which is widely associated with relatively warm conditions and sites south of treeline in training sets from the North American Arctic (e.g. Barley et al. 2006; Francis et al. 2006). In addition to suggesting warmer temperatures, the abundance of the species *C. americanus* probably indicates little to no fish predation during the early Holocene (Uutala 1990). Interestingly, both species of *Chaoborus* disappeared from the lake ~10.4 cal ka and have not returned, suggestive of a permanent environmental shift such as the arrival of fish (stickleback are currently present) in Lone Spruce Pond, or possibly a change in lake level (Uutala 1990; Barley et al. 2006).

By 10 cal ka, *Alnus* percentages reached values >20 %. This sustained high level indicates the local establishment of *Alnus* (cf. Anderson and Brubaker 1986), and differs substantially from the more sporadic peaks in pollen percentages above 15 % during the earlier record. In contrast, BSi content remained relatively low until its major shift around 8.4 cal ka.

Alnus expansion (9–8 cal ka)

During the three centuries between 8.9 and 8.5 cal ka, *Alnus* pollen in sediment from Lone Spruce Pond tripled from about 25 to 75 % (Fig. 5). By 8.4 cal ka, *Alnus* pollen reached a stable plateau around 90 %, signifying the completion of the mass expansion of the shrub around the pond. All previous pollen studies from southwest Alaska have documented a major increase in *Alnus* pollen between about 9.5 and 8.3 cal ka (Brubaker et al. 2001). Of these previously studied sites, Grandfather Lake (Hu et al. 1995, 2001) is nearest to Lone Spruce Pond, located 40 km to the southeast and 15 m higher in elevation. *Alnus* expanded about 500 years earlier at Grandfather Lake; the transformation there was about half as fast and less pronounced, with *Alnus* pollen accounting for about 75 % at Grandfather Lake compared with about 90 % at Lone Spruce Pond. The expansion of *Alnus* may have progressed westward and upward, reaching Little Swift Lake 40 km to the northwest and at 600 m elevation by about 7.5 cal ka (Axford and Kaufman 2004). And at Beaver Pond, located 275 km to the northeast (579 m asl; Kaltenrieder et al. 2011), *Alnus* expanded earlier, by about 10 cal ka, but it never dominated the pollen assemblage as it did at Lone Spruce Pond. The extent to which the expansion of *Alnus* is climatically determined is unclear. Its spread across Alaska has traditionally been attributed to cooling and moistening, possibly associated with an increase in snow (Hu et al. 1995). The time transgressiveness of the expansion suggests that other factors, such as soil preparation, migration rates, fire and even competition, may have been more important, as principal plant species continued to adjust to postglacial environments (Anderson et al. 2004).

During the two centuries following the mass expansion of *Alnus* (which culminated 8.2 cal ka), the BSi content of Lone Spruce Pond sediment nearly tripled (from 7 to 19 %). $\delta^{15}N$ increased to near-maximum values during the subsequent millennium, reflecting the buildup of N and an increase in denitrification in soils, which is known to be associated with an increase in *Alnus* (e.g. Rhoades et al. 2001). *Alnus* increases the availability of N in soils and in runoff to lakes because it is effective at fixing atmospheric N_2. The response of the BSi and N at Lone Spruce Pond was similar to that reported for Grandfather Lake (Hu et al. 2001).

The increases in *Alnus* pollen and BSi content were accompanied by an abrupt increase in Cladocera abundance and a shift in chironomid assemblage composition, including a rise in *Limnophyes,* which occurs in lakes across a large temperature gradient (Barley et al. 2006) and in a wide range of settings in the North American Arctic, including littoral and surf zones of lakes, streams, seeps, and wet tundra (Oliver and Dillon 1997); a rise in *C. ambigua*, which shows little relationship to temperature in the training set but is most abundant in shallow lakes (Barley et al. 2006); and a decline in *Micropsectra*, a taxon strongly associated with oligotrophic, well-oxygenated conditions (Brodersen

et al. 2004). Taken together, the pronounced changes in the chironomid assemblage at this time do not consistently suggest temperature change. Rather, rising percentages of both *Limnophyes* and *C. ambigua* are consistent with increasing importance of shallow-water habitat in Lone Spruce Pond, and the decline of *Micropsectra* (and subsequent rise of oxy-regulatory *Sergentia*) suggests changes in oxygen availability—two trends that could simultaneously result from changes in nutrient conditions, aquatic productivity, water quality, and lake substrate associated with the expansion of N-fixing *Alnus* within the watershed. (The increasing importance of *Limnophyes*, which is often semi-terrestrial, throughout the Holocene may also reflect the simultaneous development of surrounding peatlands.) A cascade of aquatic environmental changes resulting from the expansion of *Alnus* in the watershed is also suggested by the contemporaneous rise in BSi and changes in Cladocera abundance, which spiked about two millennia following the rise of *Alnus*. The lack of good analogs in the training set for many of the mid- to late Holocene assemblages further hampers the interpretation of the "*Alnus*" period assemblages in terms of temperature changes. These conclusions for Lone Spruce Pond are consistent with prior studies finding that major changes in vegetation or other catchment characteristics, in particular fluctuations of treeline, may influence chironomid-based temperature estimates due to associated changes in catchment soils, lake nutrient status, and other environmental conditions that influence invertebrates both directly and indirectly (Porinchu and Cwynar 2000; Velle et al. 2010).

The flux of mineral matter to the lake increased following the expansion of *Alnus* (calculated as all mass other than OM and BSi (i.e. 100 − (BSi% + OM%)), and multiplied by average density and sediment thickness for each 500-year interval). The long-term trend toward increasing sediment flux following the establishment of dense *Alnus* thickets is difficult to explain; we would hypothesize that the shrubs should have stabilized the soil. Given this unexpected result, we speculate that weathering of the hillslopes by the mechanical action of *Alnus* roots and the chemical action of increased pore-water acidification both enhanced sediment production and availability for transport to the lake after around 8 cal ka. This is consistent with the lower pH values that have been measured in soil below *Alnus* canopy compared with inter-canopy areas (e.g. Mitchell and Ruess 2009).

Post-*Alnus* expansion (8 cal ka to present)

Following the expansion of *Alnus*, all of the physical and biological properties of lake sediment at Lone Spruce Pond reached near-modern values, with some centennial-scale variability. Most noteworthy are the peaks in OM abundance (and %C) that might point to the warmest intervals of the Holocene during the centuries between around 5.5 and 4.0 cal ka, and again between 1.8 and 1.2 cal ka. These intervals of possible peak warmth do not, however, coincide with peaks in BSi. The offset between the Holocene maxima in BSi and OM probably reflects the difference in the response of the two proxies to changes in temperature versus nutrient availability, or to their response to groundwater-derived versus overland inputs. The Holocene maximum BSi content at Lone Spruce Pond took place between about 7.0 and 6.5 cal ka, which overlaps with the peak BSi content at Grandfather Lake (Hu et al. 2001), and with the peak OM content at Waskey Lake (Levy et al. 2004).

The reappearance of *Stictochironomus* after 2.4 cal ka may reflect cooler temperatures; this taxon was abundant at Lone Spruce Pond during the LGM and deglacial period but disappeared at the onset of the Holocene, and its modern distribution across Canada favors lakes in cold (arctic and alpine) climates (Walker 1990; Francis et al. 2006). *Stictochironomus* has a temperature optimum of 11.6 °C in the eastern Beringia training set, relatively cool for Chironomini and more comparable to many Orthocladiinae. During the last 2000 years, BSi and OM values were generally lower than their maximum Holocene values, with minima during the seventh and eighth centuries, and again during the eighteenth century. These periods coincide with minimum average summer temperatures reconstructed from proxy records across the Arctic (Kaufman et al. 2009). The minima were separated by an interval of peak production during the thirteenth century, which occurred about three centuries following the warmest interval in the Arctic-wide average.

Conclusions

1. Glacial-lacustrine mud (unit 1) recovered from the base of core LSP-3/4 contains plant macrofossils dating between 25 and 21 cal ka, and lacustrine microfossils (chironomids, Chaoboridae, Cladocera, and diatoms). The glacial-lacustrine sediment probably accumulated while the pond was contiguous with a higher level of adjacent Lake Chuaekuktuli. The dominant chironomid taxa suggest cool and oligotrophic—but not extremely cold—conditions. In fact, the midge assemblage includes several taxa with July air temperature optima >13 °C, albeit at low abundances. Open water at this time indicates that the Ahklun Mountain ice cap had retreated from its late Wisconsin maximum extent by >60 km, and to within 6 km of the range crest. The limited extent of ice is consistent with the midge and pollen assemblages preserved at Lone Spruce Pond at this time, with other evidence for relatively warm summers in Alaska during the global LGM, and with the output of general circulation models.
2. A possible disconformity separates the lower glacial-lacustrine mud (unit 1) from the overlying sandy mud (unit 2). The surface may record a period of erosion during which glacier ice re-advanced across the site sometime after ~21 cal ka and prior to 14.5 cal ka. The contact is marked by oxidation, and we cannot rule out the possibility that it records an interval of desiccation, nor the alternative that the dated macrofossils below the surface are reworked and that the sequence is instead conformable.
3. Non-glacial lacustrine sediment (unit 2) began accumulating in Lone Spruce Pond at 14.5 cal ka, coincident with the onset of major warming recognized elsewhere in the Northern Hemisphere. The onset of the YD at 12.8 cal ka is marked by a shift to lower BSi content, indicating a decrease in lacustrine production. BSi increased during the second half of the YD, similar to other records across southern Alaska. High sand influx throughout the late-glacial period may reflect landscape instability. Although BSi indicates that climate varied during the late glacial period, low chironomid and Cladocera concentrations combined with low sedimentation rates imply low production of aquatic invertebrates throughout this period. Midge assemblages suggest cold, oligotrophic conditions throughout.
4. Rapid local warming at the end of the YD (i.e. at the base of unit 3) is evidenced by the shift in OM content, from 10 to 30 %, paralleled by an increase in C and N abundance and C:N ratio, and a depletion in $\delta^{13}C$, all consistent with increased input of organic carbon from the surrounding watershed. At the same time, chironomid production rose and the midge assemblage changed markedly, with the addition of several relatively thermophilous chironomid and *Chaoborus* taxa suggesting abrupt warming. ^{14}C ages are too old during this interval, consistent with a flush of old dissolved organic carbon to the pond, which was incorporated into aquatic organisms used for ^{14}C dating.
5. Among the most prominent paleoenvironmental shifts at Lone Spruce Pond was that associated with the expansion of *Alnus* centered around 8.6 cal ka. Within three centuries, *Alnus* pollen percent doubled (from about 45 to 90 %), followed by a nearly three-fold increase in BSi content (8–22 %). The increase in lake production accompanying the expansion of *Alnus* indicates an increase in N availability. $\delta^{15}N$ also increased during the millennium following the expansion of *Alnus*, reflecting the gradual buildup of N in soils. The expansion of *Alnus* led to an abrupt increase in cladoceran abundance and a shift in the chironomid assemblage that likely reflect changes in lake trophic state, water quality, or other local environmental conditions. As has been observed for lakes near treeline elsewhere, major changes in local vegetation may influence Holocene paleotemperature reconstructions at some sites, but at the same time yield insights regarding the cascade of ecological changes that follow vegetation change within watersheds. Such abrupt and multifaceted paleoenvironmental changes have implications for understanding future pressures on aquatic ecosystems in the Arctic, where vegetation changes are forecast to accompany changing climate.

Acknowledgments We thank M Arnold and C Schiff for assistance in the field, and V Chavez, E Helfrich, C Schiff, K Cooper, M Nasto, D West, and staff of the Colorado Plateau Analytical Lab for their work in the laboratories. E Barley

shared her training set data and advice on midge taxonomy. M Edwards, V Markgraf and two anonymous reviewers provided helpful comments. CH2MHill Polar Services and US Fish & Wildlife Service Dillingham Office provided logistical support. This research was funded by NSF grants EAR-0823522 and -0904396 and ARC-0909332 and -0909347.

References

Abbott MB, Finney BP, Edwards ME, Kelts KR (2000) Lake-level reconstructions and paleohydrology of Birch Lake, Central Alaska, based on seismic reflection profiles and core transects. Quat Res 53:154–166

Anderson PM, Brubaker LB (1986) Modern pollen assemblages from northern Alaska. Rev Palaeobot Palynol 46:273–291

Anderson PM, Edwards ME, Brubaker LB (2004) Results and paleoclimate implications of 35 years of paleoecological research in Alaska. In: Gillespie AR, Porter SC, Atwater BF (eds) The Quaternary Period of the United States. Elsevier, Amsterdam, pp 427–440

Axford Y, Kaufman DS (2004) Late glacial and Holocene glacier and vegetation fluctuations at Little Swift Lake, southwestern Alaska, USA. Arct Antarct Alp Res 36:139–146

Barley EM, Walker IR, Kurek J, Cwynar LC, Mathewes RW, Gajewski K, Finney BP (2006) A northwest North America training set: distribution of freshwater midges in relation to air temperature and lake depth. J Paleolimnol 36:295–314

Bartlein PJ, Harrison SP, Brewer S, Connor S, Davis BAS, Gajewski K, Guiot J, Harrison-Prentice TI, Henderson A, Peyron O, Prentic IC, Scholze M, Seppä H, Shuman B, Sugita S, Thompson RS, Viau AE, Williams J, Wu H (2011) Pollen-based continental climate reconstructions at 6 and 21 cal ka: a global synthesis. Clim Dyn 37:775–802

Béget J, Mason O, Anderson P (1992) Age, extent and climatic significance of the ca. 3400 Aniakchak tephra, western Alaska. USA. The Holocene 2:51–56

Blaauw M (2010) Methods and code for 'classical' age-modelling of radiocarbon sequences. Quat Geochron 5:512–518

Briner JP, Kaufman DS (2008) Late Pleistocene mountain glaciation in Alaska: key chronologies. J Quat Sci 23: 659–670

Briner JP, Kaufman DS, Werner A, Caffee M, Levy L, Manley WF, Kaplan MR, Finkel RC (2002) Glacier readvance during the late glacial (Younger Dryas?) in the Ahklun Mountains, southwestern Alaska. Geology 30:679–682

Brodersen KP, Pedersen O, Lindegaard C, Hamburger K (2004) Chironomids (Diptera) and oxy-regulatory capacity: An experimental approach to paleolimnological interpretation. Limnol Oceanogr 49:1549–1559

Brooks SJ, Langdon PG, Heiri O (2007) The identification and use of palaearctic Chironomidae larvae in palaeoecology, QRA Technical Guide No. 10. Quaternary Research Association, London

Brubaker LB, Anderson PM, Hu FS (2001) Vegeation ecotone dynamics in southwester Alaska during the late Quaternary. Quat Sci Rev 20:175–188

Davies MH, Mix AC, Stoner JS, Addison JA, Jaeger J, Finney B, Wiest J (2011) The deglacial transition on the southeastern Alaskan Margin: Meltwater input, sea level rise, marine productivity, and sedimentary anoxia. Paleoceanogr 26: PA2223

Fægri K, Kaland PE, Krzywinski K (1989) Textbook of pollen analysis, IV edn. Blackburn Press, New Jersey

Francis DR, Wolfe AP, Walker IR, Miller GH (2006) Interglacial and Holocene temperature reconstructions based on midge remains in sediments of two lakes from Baffin Island, Nunavut, Arctic Canada. Palaeogeogr Palaeoclimatol Palaeoecol 236:107–124

Hu FS, Shemesh A (2003) A biogenic-silica $\delta^{18}O$ record of climatic change during the glacial-interglacial transition in southwestern Alaska. Quat Res 59:379–385

Hu FS, Brubaker LB, Anderson PM (1995) Postglacial vegetation and climate change in the northern Bristol Bay region, southwestern Alaska. Quat Res 43:382–392

Hu FS, Finney BP, Brubaker LB (2001) Effects of Holocene *Alnus* expansion on aquatic productivity, nitrogen cycling, and soil development in southwestern Alaska. Ecosystems 4:358–368

Hu FS, Lee BY, Kaufman DS, Yoneji S, Nelson DM, Henne PD (2002) Response of tundra ecosystem in southwestern Alaska to Younger-Dryas climatic oscillation. Glob Chan Biol 8:1156–1163

Hu FS, Kaufman DS, Yoneji S, Nelson D, Shemesh A, Huang Y, Tian J, Bond G, Clegg B, Brown T (2003) Cyclic variation and solar forcing of Holocene climate in the Alaskan subarctic. Science 301:1890–1893

Hu FS, Nelson DM, Clarke GH, Rühland KM, Huang Y, Kaufman DS, Smol JP (2006) Abrupt climatic events during the last glacial-interglacial transition in Alaska. Geophys Res Let 33:L18708. doi:10.1029/2006GL027261

Juggins S (2003) C2 User guide. University of Newcastle, Newcastle upon Tyne, UK, Software for ecological and palaeoecological data analysis and visualization

Kaltenrieder P, Tinner W, Lee B, Hu FS (2011) A 16 000-year record of vegetational change in south-western Alaska as inferred from plant macrofossils and pollen. J Quat Sci 26:276–285

Kaufman DS, Hu FS, Briner JP, Werner A, Finney BP, Gregory-Eave I (2003) A ~33,000 year record of environmental change from Arolik Lake, Ahklun Mountains, Alaska. J Paleolimnol 30:343–362

Kaufman DS, Schneider DP, McKay NP, Ammann CM, Bradley RS, Briffa KR, Miller GH, Otto-Bliesner BL, Overpeck JT, Vinther BM, Arctic Lakes 2k Project Members (2009) Recent warming reverses long-term Arctic cooling. Science 325:1236–1239

Kaufman DS, Anderson RS, Hu FS, Berg E, Werner A (2010) Evidence for a variable and wet Younger Dryas in southern Alaska. Quat Sci Rev 29:1445–1452

Kaufman DS, Young NE, Briner JP, Manley WF (2011a) Alaska Palaeo-Glacier Atlas (Version 2). In: Ehlers J, Gibbard PL (eds) Quaternary glaciations extent and chronology, part IV: a closer look. Developments in Quaternary Sciences 15, Elsevier, Amsterdam, pp 427–445

Kaufman CA, Lamoureux SF, Kaufman DS (2011b) Long-term river discharge and multidecadal climate variability inferred from varved sediments, southwest Alaska. Quat Res 76:1–9

Kaufman DS, Jensen BJL, Reyes AV, Schiff CJ, Froese DG (2012) Late Quaternary tephrostratigraphy, Ahklun Mountains, southwestern Alaska. J Quat Sci 27:344–359

Kurek J, Cwynar LC, Ager TA, Abbott MB, Edwards ME (2009a) Late Quaternary paleoclimate of western Alaska inferred from fossil chironomids and its relation to vegetation histories. Quat Sci Rev 28:799–811

Kurek J, Cwynar LC, Vermaire JC (2009b) A late Quatenary paleotemperatures record from Hanging Lake, northern Yukon Territory, eastern Beringa. Quat Res 72:246–257

Levy LB, Kaufman DS, Werner A (2004) Holocene glacier fluctuations, Waskey Lake, northeastern Ahklun Mountains, southwestern Alaska. The Holocene 14:185–193

Meyers PA, Lallier-Vergés E (1999) Lacustrine sedimentary organic matter records of late Quaternary paleoclimates. J Paleolimnol 21:345–372

Mitchell JS, Ruess RW (2009) N_2 fixing alder (*Alnus viridis* spp. *fruticosa*) effects on soil properties across a secondary successional chronosequence in interior Alaska. Biogeochem 95:215–229

Mortlock RA, Froelich PN (1989) A simple method for the rapid determination of biogenic opal in pelagic marine sediments. Deep-Sea Res 35:1415–1426

National Oceanographic and Atmospheric Administration (NOAA) (1980) Climatography of the United States. Monthly normals of temperature, precipitation, and heating and cooling degree days by state, 1951–1980

Oliver DR, Dillon ME (1997) Chironomids (Diptera: Chironomidae) of the Yukon Arctic North Slope and Herschel Island. In: Danks HV, Downes JA (eds) Insects of the Yukon. Biological Survey of Canada (Terrestrial Arthropods) Ottawa, pp 615-635

Otto-Bliesner BL, Brady ES, Tomas R, Levis S, Kothavala Z (2006) Last glacial maximum and Holocene climate in CCSM3. J Clim 19:2526–2543

Porinchu DF, Cwynar LC (2000) The distribution of freshwater Chironomidae (Insects: Diptera) across treeline near the lower Lena River, northeast Siberia, Russia. Arct Antarct Alp Res 32:429–437

Rasmussen SO et al (2006) A new Greenland ice core chronology for the last glacial termination. J Geophys Res 111:D06102. doi:10.1029/2005JD006079

Reimer PJ, Baillie MGL, Bard E, Bayliss A, Beck JW, Bertrand CJH, Blackwell PG, Buck CE, Burr GS, Cutler KB, Damon PE, Edwards RL, Fairbanks RG, Friedrich M, Guilderson TP, Hogg AG, Hughen KA, Kromer B, McCormac G, Manning S, Ramsey CB, Reimer RW, Remmele S, Southon JR, Stuiver M, Talamo S, Taylor FW, van der Plicht J, Weyhenmeyer CE (2004) INTCAL04 terrestrial radiocarbon age calibration, 0–26 cal k yr. Radiocarbon 46: 1029–1058

Rhoades C, Oskarsson H, Binkley D, Stottlemyer B (2001) Alder (*Alnus crispa*) effects on soils in ecosystems of the Agashashok River valley, northwest Alaska. Ecoscience 8:89–95

Telford RJ, Heegaard E, Birks HJB (2004) The intercept is a poor estimate of a calibrated radiocarbon age. The Holocene 14:296–298

Uutala AJ (1990) Chaoborus (Diptera: Chaoboridae) mandibles—paleolimnological indicators of the historical status of fish populations in acid-sensitive lakes. J Paleolimnol 4:139–151

Velle G, Brodersen KP, Birks HJB, Willassen E (2010) Midges as quantitative temperature indicator species: Lessons for palaeoecology. The Holocene 20:989–1002

Viau AE, Gajewski K, Sawada MC, Bunbury J (2008) Low- and high-frequency climate variability in eastern Beringia during the past 25,000 years. Can J Earth Sci 45:1435–1453

Viereck LA, Little EL Jr (2007) Alaska Trees and Shrubs, 2nd edn. University of Alaska Press, Fairbanks

Walker I (1990) Modern assemblages of arctic and alpine Chironomidae as analogues for late-glacial communities. Hydrobiologia 214:223–227

Walker I (2001) Midges: Chironomidae and related Diptera. In: Smol JP, Birks HJB, Last WM (eds) Tracking environmental change using lake sediments zoological indicators, vol 4. Kluwer, Dordrecht, pp 43–66

Western Regional Climate Center (WRCC) (2008) Dillingham FAA Airport, Alaska: Monthly Climate Summary. Available from: http://www.wrcc.dri.edu/

Wilson BF, Patterson WA III, O'Keefe JF (1985) Longevity and persistence of alder west of the tree line on the Seward Peninsula, Alaska. Can J Bot 63:1870–1875